Real Time Detection of Damage during Quasi-Static Loading of a Single Stringer Panel using Passive Thermography

Joseph N. Zalameda*[a] and Michael R. Horne[b]

[a]NASA Langley Research Center Hampton, VA 23681-2199;
[b]National Institute of Aerospace NASA Langley Research Center Hampton, VA 23681-2199

ABSTRACT

Real time nondestructive evaluation is required for composites load testing. The early detection and measurement of damage progression is important to understand failure modes. A single stringer panel was subjected to quasi-static loading to induce deformation which can result in the formation of delamination damage between the stiffener flange and skin. Passive thermography was used to detect damage in real time as a function of the applied load. The loading was stopped when damage growth was detected. Of particular interest was the early detection of damage formation which can be challenging, as compared to cyclic fatigue loading. Passive thermography data were acquired and processed in real time and revealed damaged areas due to heating from fiber breakage and delamination formation. The processed thermal imagery was also compared to acoustic emission and ultrasound data.

Keywords: Thermal nondestructive evaluation, static loading damage detection, aerospace composite inspection, passive thermography, acoustic emission, non-immersion ultrasound

1. INTRODUCTION

Real time nondestructive evaluation (NDE) is necessary for composites load testing to track early onset and growth of damage. The NDE allows for monitoring, and hence, controlling the growth of the damage as a function of the applied load. In this work, a quasi-static bending load (using seven contact points) is applied to a single stringer stiffened composite panel. When damage is detected, the loading is stopped and another inspection technique such as ultrasound or X-ray CT is used to provide a detailed assessment of the panel damage as a function of depth. When the structure is loaded to failure, real time NDE records the damage modes leading up to failure. Documentation of damage onset, growth, and panel failure provides valuable information for development and validation of progressive damage analysis (PDA) models. The ultimate goal is to use the validated PDA models to decrease the time required to test and therefore certify composite structures for aircraft thus saving development costs [1-3]. The purpose of this paper is to describe the methodology of measuring onset and damage formation/growth during quasi-static loading using passive thermography.

There have been numerous studies performed using thermography for structures testing with most applications for fatigue loading [4-9]. The challenge for passive thermography is to detect the small transient thermal signal generated by a quasi-static load as compared to the repetitive thermal signals resulting from cyclic loading. Passive thermography is different as compared to active thermography in that the addition or removal of energy is not controlled for the thermal inspection. The thermal anomalies are very small and barely detectable using a high sensitivity infrared (IR) camera and therefore a custom data acquisition system was developed to detect the small thermal signatures. The detected thermal signature is confirmed with acoustic emission. In addition, we study the timing of the acoustic emission events to areas of detected thermal anomalies. Multiple IR cameras and multiple acoustic emission sensors can be employed for large scale testing of structures, however for this effort given the panel size and setup a single thermal camera and six acoustic emission sensors were utilized.

*joseph.n.zalameda@nasa.gov; phone 1 757-864-4793; fax 1 757-864-4914; http://nde.larc.nasa.gov

2. SAMPLE DESCRIPTION AND MEASUREMENT SYSTEMS

2.1 Composite Sample Tested

The stiffened composite panel skin was 12 plies with a thickness of 0.22cm, the stiffener flange was 12 plies thick with a thickness of 0.24cm. The stiffener hat top was 16 plies with a thickness of 0.32 cm. The stiffener was a woven composite. Figures 1a, 1b, 1c, and 1d show the stiffened composite panel flat side with acoustic emission locations, stringer side, a painted specimen, and a cross sectional view respectively. The panel was painted for digital image correlation measurements to record panel deformation. Quasi-static loads were applied using seven application points, two on top (located in middle just outside of the flange) and five on the bottom (located at each corner and center). The load was applied from the bottom while the top was held stationary at two points. This configuration allowed for panel deformation that results in damage formation between the stiffener flange and skin. The applied quasi-static loads were up to 1,000 pounds. Examples of the applied load for a typical test and panel deflection are shown in Figures 2a and 2b respectively.

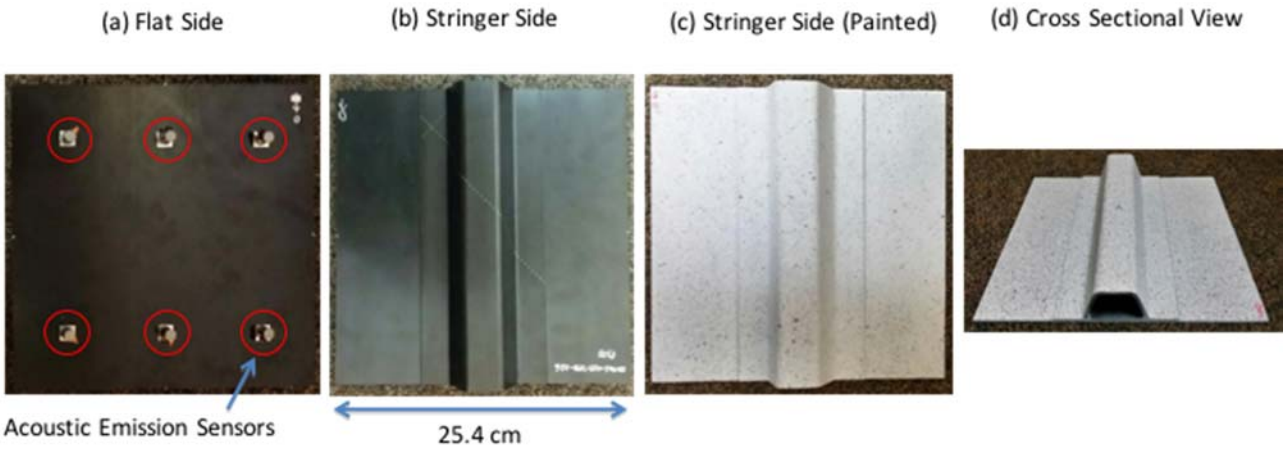

Figure 1: Single stringer composite panel with acoustic emission sensor locations.

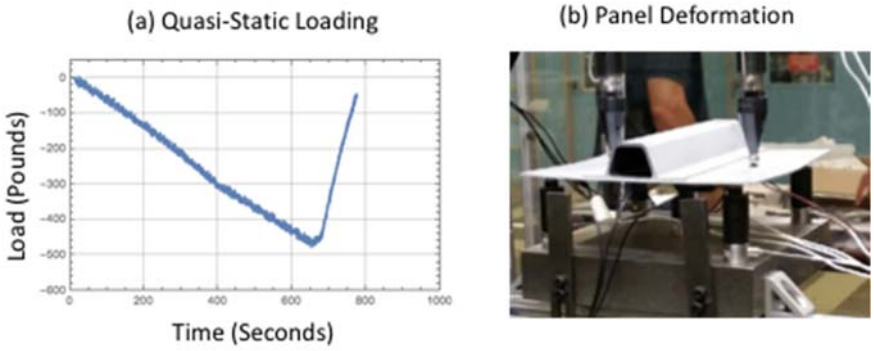

Figure 2: Applied load and panel deformation.

2.2 Passive Thermography

Passive thermography was used to track damage on the stringer side opposite the array of acoustic emission sensors mounted on the skin side. The test setup is shown in Figure 3a along with an example infrared camera view shown in Figure 3b. The basic system consists of an IR camera operating in the 3–5 micrometer IR band and an image data acquisition computer. The IR camera was configured with 25 mm germanium optics. The focal plane array size of the

camera was 640x512. The passive inspection captured the thermal variations during the quasi-static loading. The setup required a Plexiglas® shield to filter out spurious IR background sources (not shown in Figure 3a). The camera frame rate was externally triggered and operated from frequencies of 80 to 180 Hz. The load signal was also acquired using a USB based 12-bit data acquisition module. For each infrared camera frame, a load value was acquired. Furthermore, real time averaging, a delayed image subtraction, and real time contrast adjustment were used to enhance detection of the small thermal transient signatures due to the damage [9,10]. Without this processing, the faint thermal signatures that indicate early damage would be difficult to nearly impossible to detect in real time. A typical test would last 25 minutes and 50 – 60 gigabytes of thermal data would be acquired for each run. When damage is detected the loading is stopped and the sample is removed for further damage characterization using ultrasound or X-ray CT [11].

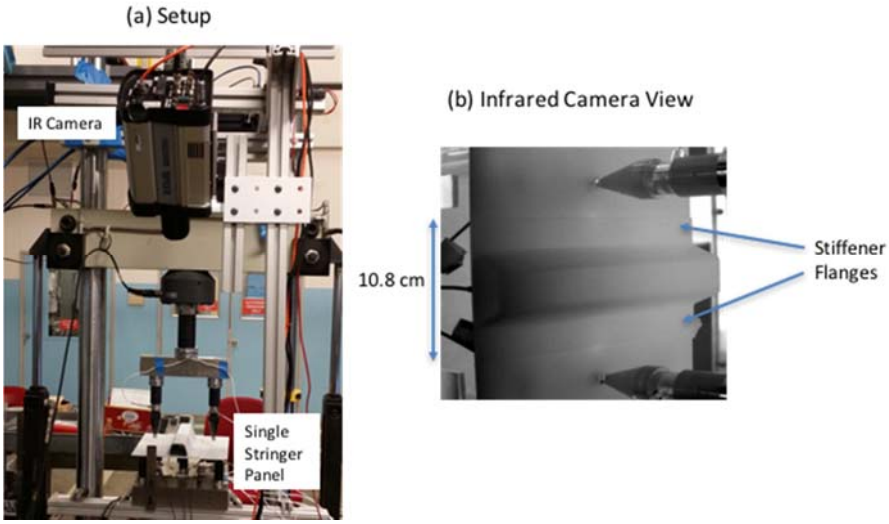

Figure 3: Quasi-static load test setup with infrared camera view.

3. MEASUREMENT RESULTS

3.1 Passive Thermography

Digital image processing was required to both enhance detection of thermal events during load and to facilitate comparison of the thermal inspection imagery to the ultrasonic data. To enhance detection in real time, image averaging and a delayed subtraction algorithm was implemented [10]. Typical parameters of 20 frames were averaged and a delay subtraction of 100 averaged frames were typically used for real time processing. The delayed subtraction removed fixed background infrared radiation while increasing sensitivity to changes. Additionally, for comparison to ultrasonic data, an image perspective transformation and a denoising algorithm were used. The image perspective transformation was used to correct for the infrared camera look angle since the optical line of sight was not normal. This is shown where the original image in Figure 4a is compared to the transformed image, Figure 4b. The image correction is performed by defining 4 points mapped to a new set of 4 desired points (normal view) [12]. Lastly, a denoising algorithm using singular value decomposition was used to remove temporal noise in the data [13]. A similar technique has been published in the past using a polynomial expression to reduce temporal temperature noise by Shepherd [14]. Although both techniques would probably give similar results, the singular value technique provides empirically determined orthogonal functions so the data reconstruction is not constrained to a polynomial function. The singular value decomposition was implemented where the thermal data A (m x n) is represented as a two-dimensional array where the number of rows (m) are the spatial locations and the columns (n) are the number of images. Singular value decomposition of A is given by the following equation:

$$A = U \Sigma V^T . \quad (1)$$

Where U is an orthogonal matrix with dimensions m x m, Σ is an mxn matrix containing the singular values, and V is an orthogonal matrix with dimension n x n. The reconstructed data matrix $A_{reconstructed}$ is determined by summation using the following equation:

$$A_{reconstucted} = \sum_{i=1}^{N} \sigma_i \, u_i \, v_i^T \tag{2}$$

where i is the index, σ_i are the are singular values of A, $u_i$are the columns of U, and $v_i$are the columns of V. N is set to 25 which gave good representation of the original data with random noise reduced. This can be seen in Figures 5a where a large heating event is detected due to the applied load. In Figure 5b the denoised image is show with improved spatial resolution to locate the flange edge. Also shown in Figure 5c is the corresponding temporal plot for a single pixel showing noise reduced considerably. This proved helpful to remove random noise in the image data exacerbated when taking the delayed subtraction. Also shown in Figure 6 is the corresponding ultrasound inspection image showing the delamination damage growing from the flange edge toward the stringer hat. The denoising algorithm allowed for better alignment with the ultrasound inspection image.

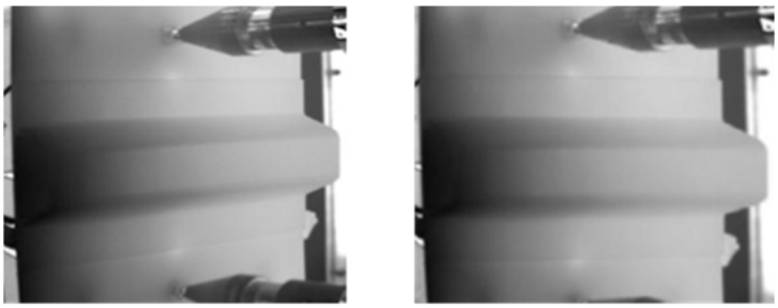

Figure 4: Comparison of original image (a) to transformed image (b) using image perspective transformation.

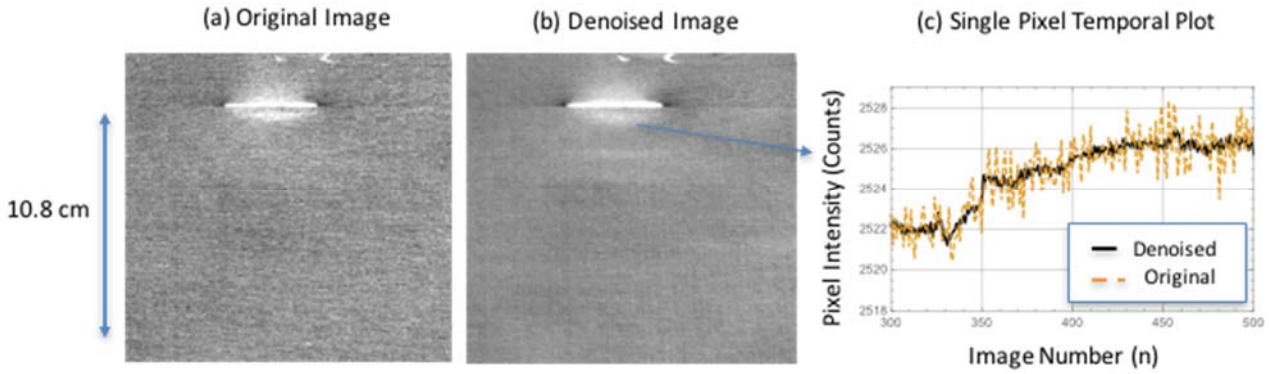

Figure 5: Comparison of original image (a) to denoised image using singular value decomposition (b), and corresponding temporal plot at a single pixel (c).

Examples of detected damage progression for a given sample during consecutive load runs are shown in Figures 7, 8, 9 and 10. The thermal damage was identified over camera noise and background reflections using three criteria: observing a bright area that appears suddenly, stays in one location, and then slowly decays in intensity over time. Using these criteria, the thermal damage is clearly identified for load runs 1 and 2 shown in Figures 7 and 9 respectively. Shown in Figures 8 and 10 are the corresponding ultrasonic inspection images. The ultrasonic inspection results show a very small edge delamination growing inward toward the stiffener hat. The thermal indications, shown in Figure 7, prove passive thermography is able to successfully detect the formation of small edge delaminations for this test setup. The thermal

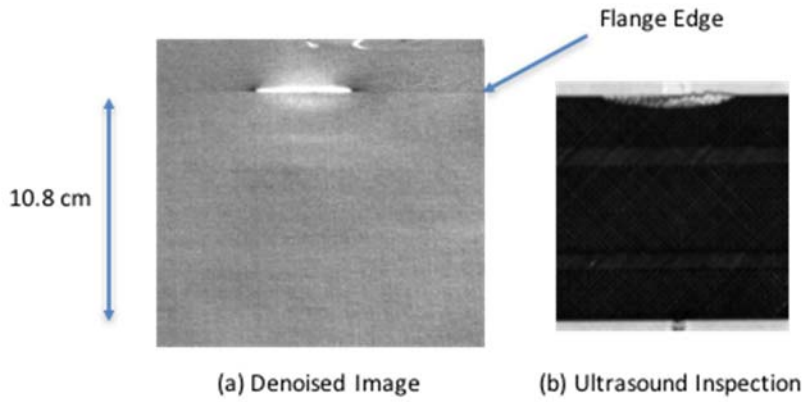

Figure 6: Comparison of denoised image (a) to corresponding ultrasound inspection image (b).

Indications from run 2 are not as pronounced as run 1, however, the small indications reveal the delamination has only grown minimally. This was confirmed with the ultrasonic inspection results shown in Figure 10. The passive thermography is able to provide the necessary information needed to control the growth of the damage thus allowing documentation with another inspection technique to determine the damage progression modes.

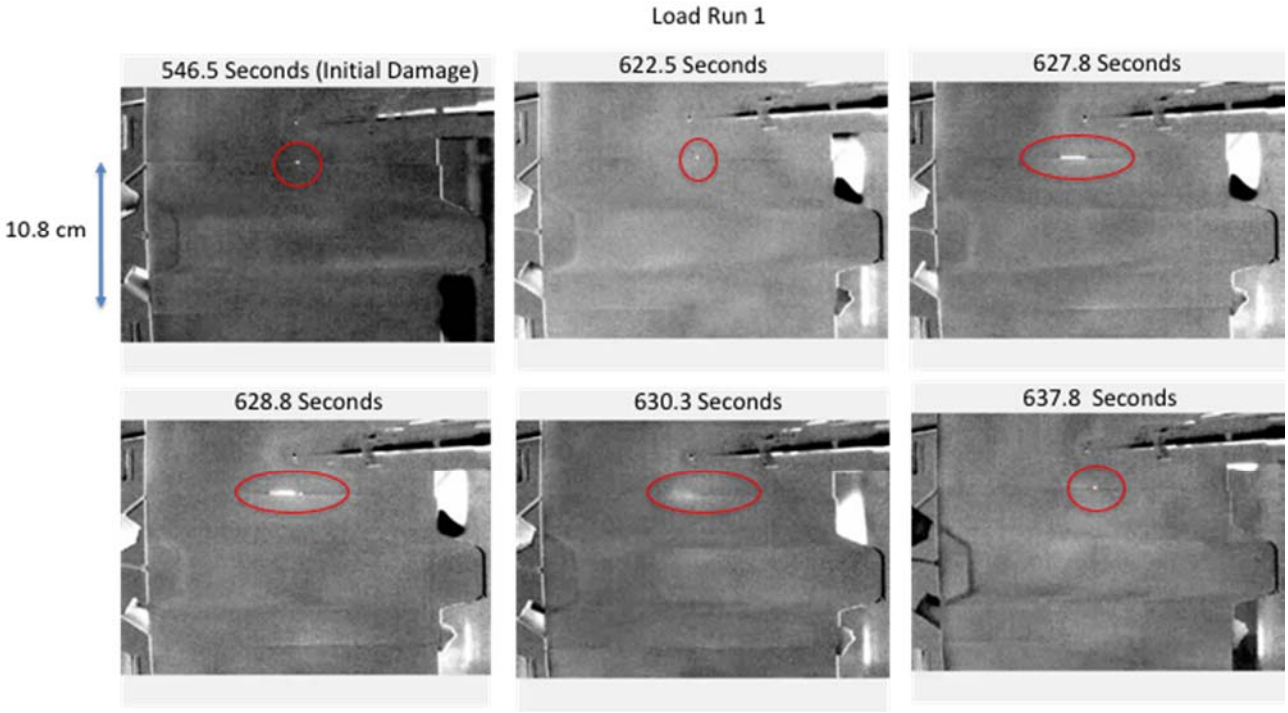

Figure 7: Processed thermal inspection images for quasi-static load run 1.

3.2 Comparison to Acoustic Emission

In addition to passive thermography, acoustic emission sensors were used to monitor damage growth in real time during each quasi-static load run [15]. The load profile is compared to the detected acoustic emission events for load runs 1 and 2 as shown in Figures 11a and 11b. When a significant number of acoustic emission events are detected along with thermal confirmation, the load profile is reversed for unloading. The total acoustic emission energy is the sum of the voltage signals detected from all six acoustic emission sensors when any one sensor crosses a set threshold. The set threshold is determined from pencil lead break calibrations performed before each load run.

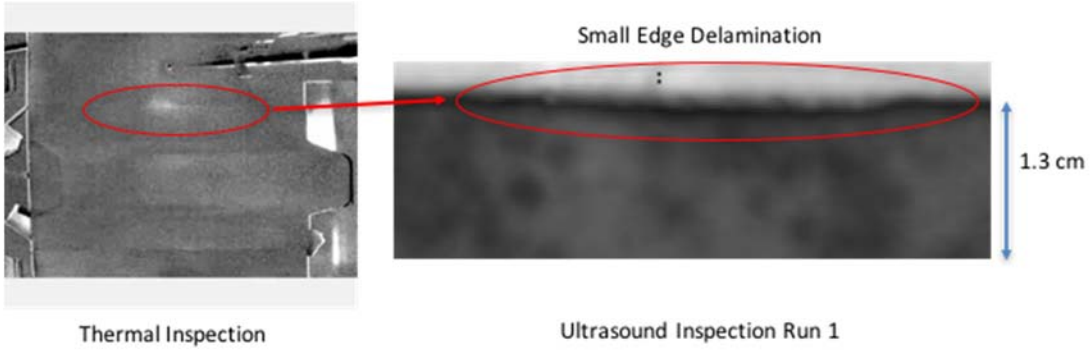

Figure 8: Comparison of thermal to ultrasonic inspection image for quasi-static load run 1.

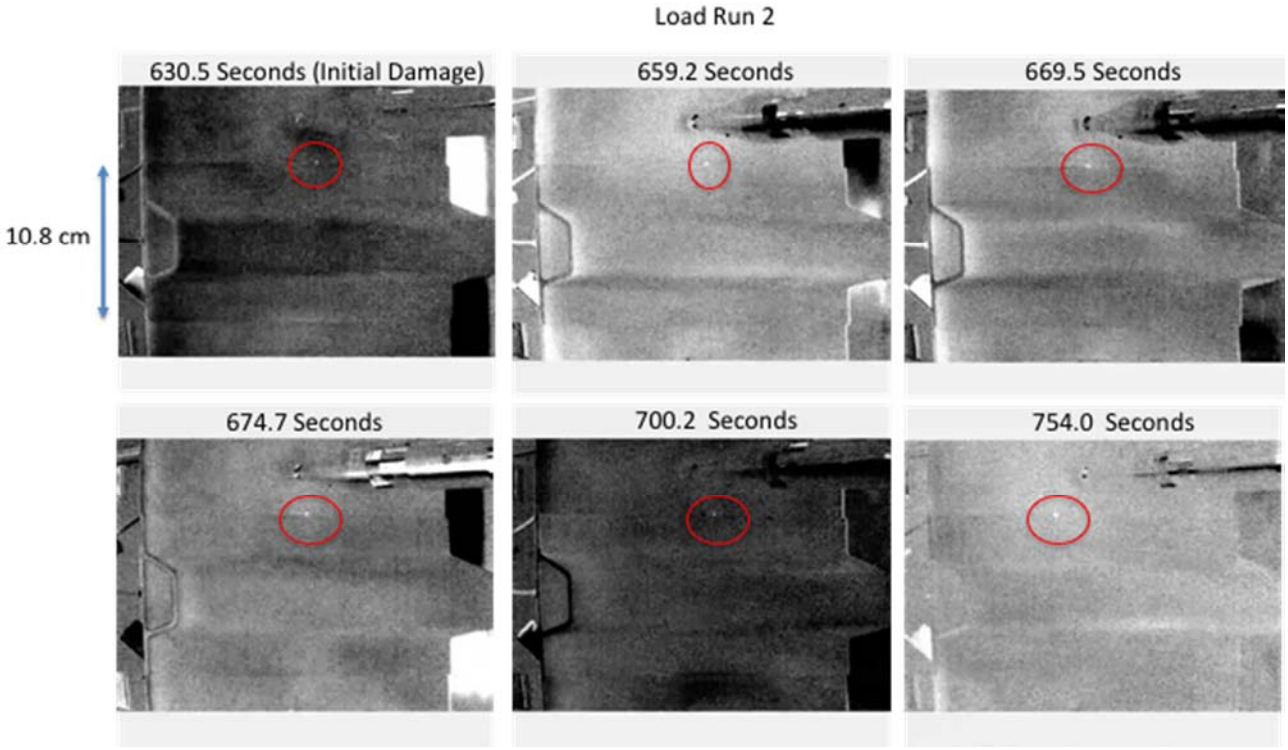

Figure 9: Processed thermal inspection images for quasi-static load run 2.

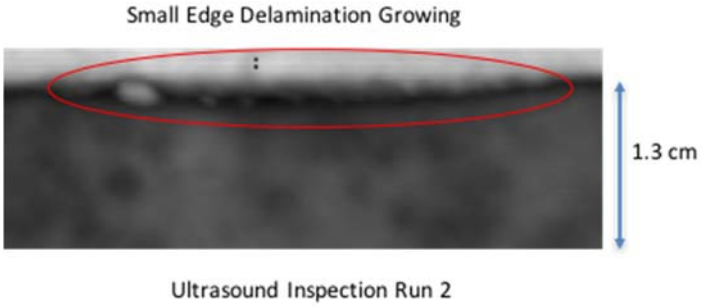

Figure 10: Ultrasonic inspection image for quasi-static load run 2 showing small delamination growth.

The acoustic emission data were compared to thermal data by aligning the recorded load profiles from each system. Shown in Figures 12a and 12b the acoustic emission events are compared to thermally detected area pixel count above a threshold of 9 counts for a given processed thermal image in time. As can be seen in Figures 12a and 12b for most of the detected acoustic emission events there is a corresponding thermal indication. Acoustic emission is sensitive to fiber break and matrix crack damage and this is expected to release some thermal energy. Acoustic emission is expected to be less dependent of damage depth, whereas for passive thermography, deeply buried damage would be more difficult to detect. Damage out of the field of view of the camera, such as damage formation under the stringer would be impossible to detect and this might account for acoustic emission events not detected thermally. For this test configuration, the array of acoustic emission sensor data was not able to provide damage location, whereas, passive thermography was able to provide damage location as shown previously in Figures 7 and 9.

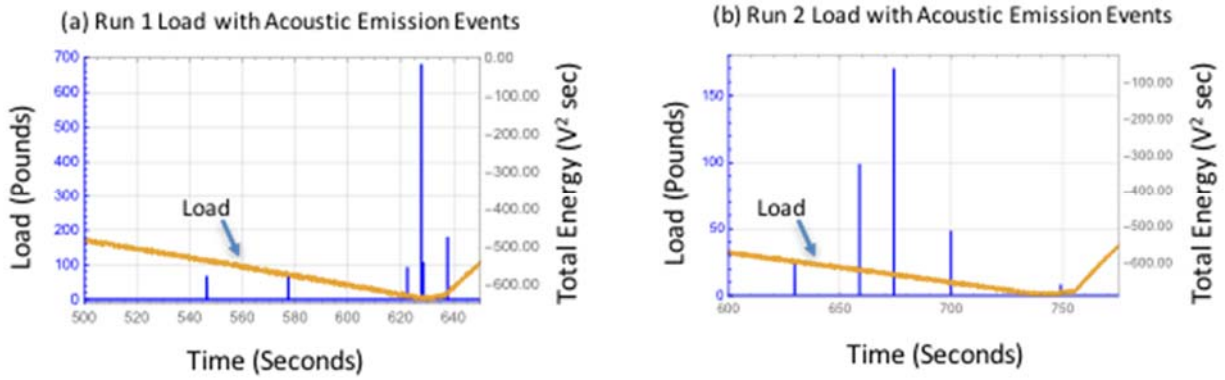

Figure 11: Comparison of load to acoustic emission events for load runs 1and 2.

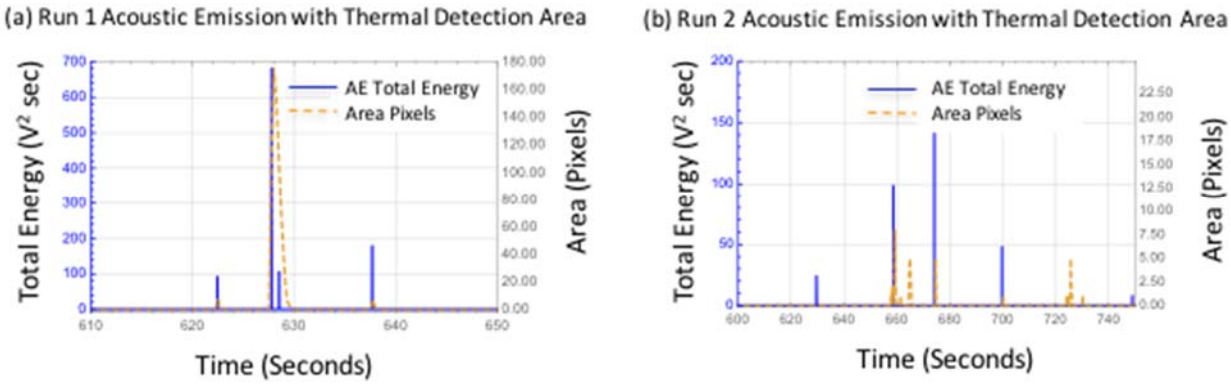

Figure 12: Detected acoustic emission events compared to thermally detected area pixels above a threshold for runs 1 and 2.

4. CONCLUSIONS

Passive thermography has been shown to be an effective real time NDE inspection technique to track damage onset and growth in a composite single stringer test panel during quasi-static loading in real time. The small thermal transient indications, detected with real time image processing, allowed for successful capture of an edge delamination onset and growth. In addition, acoustic emission data agreed well with the thermography data. For this test configuration, the array of acoustic emission sensor data was not able to provide damage location. Passive thermography was able to provide

damage location as shown previously in Figures 7 and 9. This was critical to track damage growth at a given location, to detect damage onset at a new location, or to track damage growth at multiple locations.

REFERENCES

[1] O'Brien, T. K., "Development of a Delamination Fatigue Methodology for Composite Rotorcraft Structure", NASA Aviation Safety Technical Conference Denver, CO, (October 2008).

[2] Krueger, R., "An Approach to Assess Delamination Propagation Simulation Capabilities in Commercial Finite Element Codes", NASA/TM-2008-215123, (2008).

[3] Bisagni, C., Dávila, C. G., Rose, C., and Zalameda, J. N., "Experimental Evaluation of Damage Progression in Postbuckled Single Stiffener Composite Specimens", American Society for Composites 29th Technical Conference Proceedings, US-Japan 16, ASTM D30, (February 2014).

[4] Zalameda, J. N., Burke, E. R., Parker, R. F., Seebo, J. P., Wright, C. W., and Bly, J. B., "Thermography Inspection for Early Detection of Composite Damage in Structures during Fatigue Loading", Thermosense XXXIV, edited by Douglas Burleigh, Gregory R. Stockton, Proc. of SPIE Vol. 835403 (April 2012).

[5] La Rosa, G., Clienti, T., Savio, F. Lo, "Fatigue Analysis by Acoustic Emission and Thermographic Techniques", Procedia Engineering, XVII International Colloquium on Mechanical Fatigue of Metals, (ICMFM17), Volume 74, pp. 261-268, (2014).

[6] E. Kordatos, K. Dassios, D. Aggelis, T. Matikas, "Rapid evaluation of the fatigue limit in composites using infrared lock-in thermography and acoustic emission", Mechanics Research Communications, 54, pp. 14–20, (2013).

[7] Munoz, V., Vales, B., Perrin, M., Pastor, M. L., Welemane, H., Cantarel, A., and Karama, M., "Damage detection in CFRP by coupling acoustic emission and infrared thermography", Composites Part B: Engineering, Volume 85, pp. 68-75, (February 2015).

[8] Ringermacher H. I., et al, "System and Method for Locating Failure Events in Samples Under Load", United States Patent No. 7,516,663 B2, (April 14, 2009).

[9] Zalameda, J. N., Burke, E. R., Horne, M. R., and Madaras, E. I., "Large Area Nondestructive Evaluation of a Fatigue Loaded Composite Structure", Residual Stress, Thermomechanics & Infrared Imaging, Hybrid Techniques and Inverse Problems, Vol. 9, Proceedings of the 2016 Annual Conference on Experimental and Applied Mechanics, ISBN 978-319-42254-1, Chapter 4, (2017).

[10] Winfree, W. P., Zalameda, J. N., and Howell, P. A., "Improved flaw detection and characterization with difference thermography", Proc. SPIE 8013, 80130U (April 2011).

[11] Johnston, P. H., Wright, C. W., Zalameda, J. N., and Seebo, J. P., "Ultrasonic monitoring of ply crack and delamination formation in composite tube under torsion load", Ultrasonic Symposium (IUS), IEEE, pp. 595 – 598, (2010).

[12] Chan, M., (published 2012, March 09), "Perspective Control/Correction", Retrieved from URL https://www.mathworks.com/matlabcentral/fileexchange/35531-perspective-control--correction (downloaded Jan. 2018).

[13] Hourigan, J. S., and McIndoo, L. V., "The Singular Value Decomposition." Dec. 1998. College of the Redwoods.

[14] Shepherd, S. M., "System for generating thermographic images using thermographic signal reconstruction", United States Patent No. US6751342B2, (December 2, 1999).

[15] Horne, M. R. "Rayleigh Wave Acoustic Emission during Crack Propagation in Steel". PhD Dissertation, Virginia Polytechnic Institute and State University. (2003).